pH-sensitive polymeric nanoparticles with antioxidant and anti-inflammatory properties against cisplatin-induced hearing loss

Sergio Martín-Saldaña[1, 2], Raquel Palao-Suay[1,3], María Rosa Aguilar[1,3*], Luis García-Fernández[1], Humberto Arévalo[1], Almudena Trinidad, Rafael Ramírez-Camacho[2], Julio San Román[1,3].

[1] Grupo de Biomateriales, Departamento de Nanomateriales Poliméricos y Biomateriales, Instituto de Ciencia y Tecnología de Polímeros, ICTP-CSIC, C/ Juan de la Cierva, 3, 28006 Madrid, España.

[2]Ear Research Group, Hospital UniversitarioPuerta de Hierro Majadahonda, Health Research Institute Puerta de Hierro, Madrid, Spain

[3]Networking Biomedical Research Centre in Bioengineering, Biomaterials and Nanomedicine, CIBER-BBN, Spain

KEYWORDS: anti-inflammatory; antioxidant; ototoxicity; nanoparticles; dexamethasone; ibuprofen

ABSTRACT

Polymeric nanoparticles (NP) based on smart synthetic amphiphilic copolymers are used to transport and controlled release dexamethasone in the inner ear to protect against the ototoxic effect of cisplatin. The NP were based on a mixture of two pseudo-block polymer drugs obtained by free radical polymerization: poly(VI-co-HEI) and poly(VP-*co*-MVE) or poly(VP-*co*-MTOS), being VI 1-vinylimidazole, VP *N*-vinylpyrrolidone, and IBU, MVE and MTOS the methacrylic derivatives of ibuprofen, α-tocopherol and α-tocopheryl succinate, respectively. The NP were obtained by nanoprecipitation with appropriate hydrodynamic properties, and isoelectric points that matched the pH of inflamed tissue. The NP were tested both *in vitro* (using HEI-OC1 cells) and *in vivo*(using a murine model) with good results. Although the concentration of dexamethasone administered in the nanoparticles is around two orders of magnitude lower that the conventional treatment for intratympanic administration, the NP protected from the cytotoxic effect of cisplatin when the combination of the appropriate properties in terms of size, zeta potential, encapsulation efficiency and isoelectric point were achieved. To the best of our knowledge this is the first time that pH sensitive NP are used to protect from cisplatin-induced hearing loss by intratympanic administration.

INTRODUCTION

Nanomedicine represents one of the most attractive tools to develop new therapies to effectively reach the inner ear[1]. In this sense, polymer therapeutics, and more specifically polymer drugs (a polymer where a drug has been covalently attached), offer the opportunity to obtain bioactive macromolecules with improved pharmacological properties and can be designed with amphiphilic properties that give rise to the formation of micelles or vesicles through self-assembled mechanisms. These polymeric nano-assemblies have several advantages if compared to other traditional treatments. Particularly, the core of the polymeric nanoparticles (NPs) can be used to encapsulate hydrophobic drugs, improving their bioavailability, decreasing their toxicity and protecting them from degradation processes[2].

However, one of the most relevant limitations of NPs drug delivery systems is their poor cellular internalization that significantly reduces the intracellular dosages of drugs to the level below the therapeutic window[3].In this sense, intelligent-responsive delivery systems have opened the possibility to counteract this limitation [4, 5].Among the different types of stimuli, pH-responsiveness is one of the most frequently used to design nano-system for drug delivery for the treatment of inflamed tissues where the pH is ranged from 5.5 to 6.8 as a result of the high rate of glycolysis and an increase in lactic acid concentration in affected cells, averaging 0.2– 0.6 units lower than mean extracellular pH of normal tissues [6]. Additionally, significant differences can be also found in the pH into different cellular organelles. For instance, pH of endosome and lysosome are even lower than 5.5. This is particularly relevant in the case of polymeric NPs, which are frequently uptake by endocytosis within endosomal and lysosomal compartments[7, 8].

Inflammation and reactive oxidative species (ROS) accumulation are closely related to cisplatin (CDDP) induced apoptosis of cochlear cells, which leads to a severe hearing loss[9, 10]. In spite of serious side effects related to the treatment with high doses (up to 80 mg/m^2) of CDDP, the platinum-based cytostatic is still being used due to its high efficacy in the treatment of several solid tumors, such as non-small cell lung cancer [11]or testicular cancers[12]. Over 60% of pediatric patients developed irreversible hearing loss when treated with CDDP, which delays educational and psychosocial development [13].

CDDP efficacy against tumor cells is principally due to DNA damage which leads to apoptosis. Although, cochlear and stria vascularis cells have low rates of proliferation and they are prone to CDDP-induced apoptosis. One of the major causes of CDDP-induced ototoxicity is related to ROS generation[9]. Although, the mechanism which describes ROS-induced cytotoxicity of cochlear cells remains unclear, all the mechanisms previously described of CDDP-induced ototoxicity involves oxidative stress. For example, NADPH oxidase 3 (NOX3), which is highly expressed in cochlear cells is a major source of ROS and leads to inflammation and cell death after CDDP treatment, which results in hearing loss[14].

The design of an effective pH sensitive drug delivery system for the effective treatment of associated inflammatory process related to CDDP-induced ototoxicity is an important goal of our society. In this sense, our group has extensive experience in the preparation of nanovehicles to transport toxic and hydrophobic anticancer and anti-inflammatory drugs[15-17].

On the one hand, α-tocopheryl succinate (α-TOS) is a well-known mitocan (mitochondially targeted anticancer compound) with demonstrated anticancer and antiangiogenic properties[18, 19]. α-TOS selectively induces apoptosis of cancer cells and apoptosis of proliferating endothelial cells by the increase of ROS levels and induction of the intrinsic pathway of apoptosis[20]. Our group has recently described the synthesis and biological activity of bioactive NPs based on copolymeric systems of *N*-vinylpyrrolidone (VP) and methacrylic derivatives of α-TOS and α-tocopherol (MTOS and MVE, respectively).[21]. These polymeric formulations demonstrated their potential as nanocarriers for drug delivery to the inner ear, reducing CDDP-induced ototoxicity *in vitro* and *in vivo* by the encapsulation of 6α-methylprednisolone (MP) or dexamethasone (Dx) in the inner core of the NPs[2, 22]. Moreover, recent studies by Kim et al. [23]support the effectiveness of α-TOS acting as ROS scavenger in CDDP-induced cytotoxicity in the auditory cell line HEI-OC1 resulting in a significant reduce of apoptosis.

Alternatively, ibuprofen is one of the most commonly used non-steroidal anti-inflammatory drug (NSAIDs) for the treatment of inflammatory diseases in our society. However, the use of NSAIDs for the treatment of associated inflammatory process involved to CDDP-induced ototoxicity has not successfully explored yet. Particularly, Li et al. demonstrated that the use of aspirin and other NSAIDs can cause temporary hearing

loss. Nevertheless, there is no evidence at present that ibuprofen triggers ototoxicity and, for that reason, its pharmacological effect as anti-inflammatory agent could be quite attractive to palliate the inflammatory events that produces the administration of CDDP [24].Due to the quite hydrophobicity of ibuprofen and therefore its difficult effective administration, Suarez et al. synthesized amphiphilic copolymer based on a methacrylic derivative of ibuprofen (HEI) and 1-vinylimidazol (VI)[25]. In fact, VI was selected due to its hydrophilicity, pH sensitivity (pKa of VI is around 6)[26]. However, the pKa of synthesized copolymers was too low for their application in an inflammatory microenviroment.

For that reason, the aim of this work was the synthesis, characterization, *in vitro* and *in vivo* evaluation of new pH-sensitive NPs with antioxidant and anti-inflammatory properties by the combination of amphiphilic bioactive copolymers based on methacrylic derivatives of α-TOS and HEI with the mentioned properties.The copolymers will form surfactant-free self-assembled NPs by nanoprecipitation that will be able to encapsulate Dx which could ameliorate CDDP-induced apoptosis in the inner ear.

Several authors have combined different copolymers in a single polymeric nanocarrier with and without pH sensitivity due to the several advantages of this strategy[27]. Pluronic[28, 29], polyesters[30, 31] and polypeptides[32, 33] are the most researched polymeric materials used to form blend nanocarriers for their use in drug delivery applications. Recently, the addition of vitamin E derivatives[34] as D-α-tocopheryl polyethylene glycol succinate (TPGS)[35] or modified phospholipids[36] has been also reported in the literature.

In the majority of the mixed micelles, the combination of different copolymers has been related to the improvement of the critical micelle concentration, size, *in vivo* bioavailability and drug loading capacity[27]. For that reason, mixed NPs have been used to effectively encapsulate different hydrophobic drugs such as a wide range of anticancer drugs or diverse corticoids. In this sense, the co-delivery of both types of hydrophobic molecules in a single nanoparticulate system has been recently described in the literature. This strategy can guarantee the simultaneous delivery of drug and provide advantages over the combination of the single administration of the free drugs[37]. For example, Bin et al. encapsulated methyl prednisolone and minocycline in the core of poly(lactide-*co*-glycolic acid) (PLGA) NPs for improved post-traumatic spinal cord injury conditions in rats[38]. In the same way, Li et al. investigated combined the release of dapsone and

clofazimine from PLGA NPs for improved therapeutic efficacy against tuberculosis in rats[39]. Finally, Duan et al. prepared a smart pH-sensitive and temporal-controlled polymeric micelles for the effective combination therapy of doxorubicin and disulfiram[40]. In spite of all these previous studies, the combination of ibuprofen and dexamethasone to decrease ototoxicity of CDDP and their related inflammatory event will be described for the first time in this work.

In this work, new HEI-based polymeric systems (poly(VI-*co*-HEI))were synthesized[21]and properly combined with poly(VP-*co*-MTOS) or poly(VP-*co*-MVE) in order to obtain self-assembled NPs with optimal properties regarding to size, charge and isoelectric point (pI), in order to favor VI ionization in the slightly acid environment of the tissue due to ROS increase and inflammation generated by CDDP treatment and induce the release of the encapsulated active compound in the inner ear. This is the first time that a pH sensitive polymeric system is used against cisplatin-induced hearing loss.

MATERIALS AND METHODS

Reagents and monomers

Dimethylsulfoxide (DMSO, Scharlau) was used without further purification and 2,2'-azobisisobutyronitrile (AIBN, Merck) was recrystallized from methanol for the preparation of amphiphilic copolymers. Deuteraded DMSO (DMSO_d_6, Merck) and chromatographic grade dimethylformamide (DMF, Scharlab) were used without further purification to characterize polymeric systems. Additionally, 1,4-dioxane (Panreac), tetrahydrofuran (THF, Scharlau), ethanol (EtOH, Merck), phosphate buffered solution at pH 7.4 (PBS, Sigma-Aldrich), coumarin-6 (c6, Sigma-Aldrich), dexamethasone (Dx, Sigma-Aldrich) and α-tocopheryl succinate (α-TOS, Sigma-Aldrich) were used without further purification to prepare self-assembled NP. Finally, CDDP (1 mg/ml) was purchased from Accord Healthcare (Barcelona, Spain).

N-vinyl pyrrolidone (VP, Sigma-Aldrich) was purified by distillation under reduced pressure and1-vinylimidazole (VI, Sigma-Aldrich) was used without further purification. The methacrylic derivatives of ibuprofen (HEI), α-tocopherol (MVE) and α-tocopheryl succinate (MTOS)were synthesized as described previously by our group elsewhere[25][21].

Characterization techniques

^{1}H-NMR and ^{13}C-NMR were performed in a Mercury 400BB apparatus, operating at 400 and 100 MHz, respectively. The spectra were recorded by dissolving the corresponding sample in deuterated DMSO-d_6 at 25 ºC. Fourier transform infrared attenuated total reflectance (FTIR-ATR) spectroscopy was performed in a Perkin Elmer Spectrum One FTIR spectrometer using 32 scans, and a resolution of 4 cm^{-1}.Glass transition temperatures (T_g) were determined by differential scanning calorimetry with a Perkin Elmer DSC7 interfaced to a thermal analysis data system TAC 7/DX. The dry samples (10-15 mg) were placed in aluminium pans and heated from -30 to 120 ºC at a constant rate of 10°C/min. T_g was taken as the midpoint of the heat capacity transition. The average molecular weight (M_n and M_w) and polydispersity (M_w/M_n) of all the polymers were determined by size exclusion chromatography (SEC), using a Perkin-Elmer Isocratic LC pump 250 coupled to a refraction index detector (Series 200). Two Resiporecolumns (250 mm x 4.6 mm, Varian) were used as solid phase, and degassed DMF (0.3 mL/min) with LiBr (0.1 % w/v) was used as eluent and temperature was fixed at 70ºC. Monodisperse poly(methyl methacrylate) standards (Scharlab) with molecular weights between 10.300

and 1.400.000 Da were used to obtain the calibration curve. Data were analyzed using the Perkin-Elmer LC solution program.

Synthesis of amphiphilic copolymers

Poly(VP-*co*-MVE) and poly(VP-*co*-MTOS) with a copolymer molar composition of VP:MVE 60:40 and VP:MTOS 89:11 (from now on MVE and MTOS, respectively) were synthesized as recently described by our group[21]. Additionally, two newly copolymers based on VI and HEI were obtained by free radical polymerization with copolymer molar compositions of VI:HEI (94:6) and (86:14) (from now on HEI6 and HEI14), according to the procedure previously described by our group[25].

Synthesis of polymeric NPs

Self-assembled NPs were synthesized by nanoprecipitation [41].MTOS or MVE and HEI6 or HEI14 (10 or 20 % w/w) were dissolved in THF:EtOH (50:50 v/v) at a concentration of 50 mg/mL. In the case of loaded NPs, Dx or c6 (10/15 % and 1% w/w respect to the polymer) was dissolved in THF and added to polymer solution. Afterwards, the organic solution was added drop by drop over PBS under constant magnetic stirring to obtain a final polymer concentration of 2.0 mg/mL. After the nanoprecipitation, milky NP dispersions were dialyzed against PBS during 72 h in order to remove the organic solvent and unloaded Dx or coumarin-6. NP suspension was sterilized by filtration in an aseptic environment through 0.22 μM polyethersulfone membranes (PES, Millipore Express®, Millex GP) and stored at 4 ºC before biological studies.

- *Dx and c6 encapsulation efficiency*

The encapsulation efficiency (EE) was defined as the ratio of detected experimentally and original amount of c6 or Dx encapsulated in the inner core of the NPs. Particularly, Dx and c6-loaded NPs were freeze dried in order to eliminate the aqueous phase, obtaining an amorphous powder in both types of NPs with a yield higher than 90 %. The freeze-dried NPs were dissolved in 2 ml of chloroform over 24 hours. After that, ethanol was added over 24 hours to precipitate the polymers. Samples were centrifuged at 10.000 rpm and supernatants were analyzed by absorbance or fluorescence spectroscopy, respectively. Dx absorbance was measured at 239 nm using a Perkin Elmer Lambda 35 UV/VIS spectrophotometer. Fluorescence of c6 was quantified with an excitation

wavelength of 485 nm and a maximum emission of 528 nm using a Biotek SYNERGY-HT plate reader.

Characterization of polymeric NPs

The morphology of NPs was observed using scanning electron microscopy (SEM) with a Hitachi SU8000 TED, cold-emission FE-SEM microscope working at 25 kV. Samples were prepared by deposition of one drop of the corresponding NP suspension over small glass disks and evaporation at room temperature.

The particle size distribution of the NP suspensions was determined by dynamic light scattering (DLS) using a Malvern Nanosizer NanoZS Instrument equipped with a 4mW He-Ne laser (λ=633 nm) at a scattering angle of 173º and 25 ºC. The zeta potential of NP dispersions was measured by laser Dopper electrophoresis (LDE). NP formulations were prepared at 0.4 mg/mL in a saline solution (NaCl 100 mM) and diluted 1:10 to reduce the excessive amount of ions. The pI values of different NP formulations were calculated when their zeta potential is zero. The pH of NP dispersions was changed by acid-base titration using aqueous solutions of HCl (1M) and NaOH (0.1 M) .

In vitro c6 and esterase-mediated Dx releasec6-loaded NPs were prepared in 10 mL of saline solution (NaCl, 100 mM), obtaining a neutral pH. Afterwards, pH was varied with HCl and NaOH (0.1 N) under magnetic stirring at room temperature. At desired pH values, the fluorescence intensity of c6 was quantified by fluorescence spectroscopy ($\lambda_{excitation}$= 485 nm and $\lambda_{emission}$ = 528 nm) using a Biotek SYNERGY-HT plate reader and the size of NPs was evaluated by DLS as it was previously described.

5 mL of Dx-loaded NPs (MVE-HEI14-10Dx, MTOS-HEI14-10Dx) with 15 u/mL of porcine liver esterase (Sigma-Aldrich) were dialyzed against 10 mL of PBS at 37 °C (Spectrum Laboratories, 3.5 kDa molecular weight cut-off). After certain periods, 1 mL of the dialysis medium was withdrawn and the same volume (1 mL) of PBS was replenished. Dx concentration was measured by HPLC (Shimadzu). The separation was performed on a C18-column (4.6 mm × 250 mm, Agela Technologies) at 30°C. The mobile phase was a mixture of acetonitrile, and distillated water (80:20, v/v) pumped at a rate of 1 mL/min. The UV detector was set at λ_{abs} =239 nm for Dx. The calibration curve, y = 11627x + 32761 (r^2=0.998), showed linearity between 125 µg/ml and 1.95 µg/ml being the limit of detection (LOD) and limit of quantitation (LOQ) of Dx 0.16

μg/ml and 0.49 μg/mL, respectively, according to the International Conference on Harmonization guidelines. The experiment was carried out in triplicate.

In vitro biological activity

- *Cell culture*

The HEI-OC1 cell line was a kind gift from Dr. Federico Kalinec (House Ear Institute, Los Angeles, CA). HEI-OC1 cells were maintained over permissive conditions in high-glucose Dulbecco's modified Eagle's medium (DMEM; Sigma, Saint Louis, MO, USA) supplemented with 10% fetal bovine serum (FBS; Gibco, BRL), 5% L-Glutamine (Sigma, Saint Louis, MO, USA) and Penicillin-G (Sigma, Saint Louis, MO, USA) at 33 °C in a humidified incubator with 10% CO_2.

- *NPs toxicity and cytoprotection assay*

3000 cells/well were seeded in a 96 well-plate under permissive conditions. Cells were exposed to different concentrations of NPs suspension (2.00, 1.00, 0.50, 0.25 and 0.12 mg/ml) and viability was determined by AlamarBlue® (Invitrogen). To measure NPs cell protection against CDDP, cells were treated under the same concentrations of NPs and 30 μM CDDP for the period of 24 hours in DMEM without FBS to avoid uncontrolled cell growth. CDDP was added 4 hours after NPs administration to allow the NPs internalization by the cells. These conditions simulate the real treatment as the NPs will be more efficient if administered in advance, before CDDP. The NPs will reach and protect the therapeutic target before the antitumor drug.

<u>Biochemical assays</u>

- *Caspase-3/7 activity measurement*

$2x10^5$ cells/ml were seeded and after 24 h of incubation, 0.25 mg/ml of NPs were added and after 4 hours 20 μM CDDP was added to each well. CDDP-induced caspase-3 activation was measured 16 hours after CDDP addition with the colorimetric assay EnzChek® Caspase-3 Assay Kit #2 (Molecular Probes, Inc) following the manufacturers protocol.

- *Interleukin IL-1β release*

$2x10^5$ cells/mL were seeded and after 24 hours cells were treated with different NPs formulations at 0.25 mg/ml, 4 hours after that, a final concentration of 20 μM CDDP was

added to each well. 24 hours after CDDP-induced, IL-1β release was measured by ELISA IL-1β mouse kit (BioSource International, Camarillo, CA) following the manufacturers protocol.

- *Reactive Species Quantification (Total ROS/RNS)*

Total ROS/RNS free radical activity was measured by the OxiSelect *in vitro* ROS/RNS Assay Kit. Supernatants of HEI-OC1 cultures, after being in contact with PBS, NPs, CDDP or NPs and CDDP (50 μL each), were added to the wells with 50 μL of a catalyst included in the kit (diluted in PBS at 1:250) in order to accelerate the oxidative reaction. After a brief incubation, 100 μL of the prepared DCFH probe was added to each well. The samples were measured fluorometrically against DCF standard and free radical content was determined by comparison with the predetermined DCF curve. Relative fluorescence was Multi-Detection Microplate Reader Synergy HT (BioTek Instruments; Vermont, USA) at 480 nm excitation/530 nm emission.

In vivo experiments

Sixteen healthy Wistar rats weighting 180-280 g were used. All animals were housed in plastic cages with water and food available *ad libitum,* and maintained on a 12 h light/dark cycle. Rats with signs of present or past middle ear infection were discarded. Animals were randomly assigned to different groups (**table S1, see Supporting Information**). The animals were handled according to the guidelines of the Spanish law for Laboratory animals care registered in the "Real Decreto 53/2013" and the European Directive 2010/63/EU. The study was approved by the Clinical Research and Ethics Committee of the University Hospital Puerta de Hierro (PROEX 022/16).

An initial auditory steady-state responses (ASSR) test was performed on all anesthetized animals. An insert earphone (Etymotic Research ER-2) was placed directly into the external auditory canal. Subcutaneous electrodes were placed over the vertex (active) and in the pinna of each ear (reference). Ground electrodes were placed in the right leg muscles. ASSR were recorded using an evoked potential averaging system (Intelligent Hearing System Smart-EP) in an electrically shielded, double-walled, sound-treated booth in response to 100 ms clicks or tone burst at 8, 12, 16, 20, 24, 28, 32 kHz with 10 ms plateau and 1 ms rise/fall time. Intensity was expressed as decibels sound pressure

level (dB SPL) peak equivalent. Intensity series were recorded, and an ASSR threshold was defined by the lowest intensity able to induce a replicable visual detectable response.Following the ASSR measurements the right ear bulla was surgically approached and openedand 50 µl of NPs suspension were injected in the middle ear by bullostomy using a spinal needle (BD Whitecare 27G). Left ear was injected with PBS through the bullostomy as a control. After injection the anesthetized animals remained in lateral decubitus for 30 min to maximize the suspension's contact time with the RWM and to prevent its leakage into the pharynx through the Eustachian tube.

After surgery, enrofloxacin and morphine (Braun 20 mg/ml) were administered subcutaneously for prevention of infection and postoperative analgesia, respectively. In the case of CDDP-treated groups, after NPs administration in the right ear, an intraperitoneal slow infusion of CDDP (10 mg/kg) was carried out for 30 min. After CDDP infusion, animals were housed in individual cages with *ad libitum* access to water and food. ASSR were tested after 3 days, and rats were euthanized by CO_2 suffocation.

- *In vivo distribution of c6-loaded NP*

c6-loaded NPs based on MTOS-H14 were administered *in vivo* as described in the previous section. However, these animals were euthanized after 2h to achieve NPs ability to diffuse over RWM. Cochlea was extracted and fixed in paraformaldehyde over 24h and decalcified in 1 % ethylenediaminetetraacetic acid (EDTA) at room temperature (with daily changes) for 10–12 days. Once the bone was completely decalcified, the cochlea was bisected along a mid-modiolar plane and the half-turns cut apart, and the pieces of tissue were mounted on a microscope slide.Samples were visualized using a confocal laser fluorescence microscope (CLFM; Leica TCS-SP5 RS AOBS).

Statistical analysis

One-way ANOVA was used to analyze for statistical significance of all *in vitro* and *in vivo* results. Tukey test was used to identify significant differences between the paired treatments. $p<0.05$ was considered statistically significant.

RESULTS AND DISCUSSION

Description and characterization of copolymeric systems

The combination of two different copolymeric drugs was carried out in order to provide multiple functionalities to NPs. Antioxidant properties were obtained by the presence of copolymer drugs with methacrylic derivatives of α-TOS and α-tocopherol (MTOS and MVE) and the pH sensitivity and anti-inflammatory activity were obtained by the incorporation of polymeric systems based on VI and the methacrylic derivative of ibuprofen (HEI).

Between all the NPs based on the poly(VP-*co*-MTOS) and poly(VP-*co*-MVE) family described by Palao et al., those with a copolymer molar composition of VP:MTOS 89:11 and VP:MVE 60:40 (from now, MTOS and MVE) presented the highest bioactivity and therefore, these copolymers were used in the synthesis of the new NPs[21]. Between all the copolymers described by Suarez et al. [25] all of them presented anti-inflammatory properties, but none of them presented an optimum pK_a for our application. For that reason, new copolymer drugs with a copolymer molar compositionof VI:HEI(94:6) and (86:14) (from, now, HEI6 and HEI14, respectively)were synthesized by free radical polymerization in order to fit the pK_a of the copolymer to the acidic pH of the CDDP-induced inflammatory environment in the inner ear (between 5.5 and 6.8). ^{1}H NMR spectra are shown in **figure S1** (see Supporting Information).

Table 1 summarizes the most relevant characteristics of different selected copolymeric systems. In all cases, amphiphilic pseudo-block copolymers were successfully obtained with copolymer molar composition of methacrylic derivatives slightly different from the initially feed molar composition. This is due to the difference on the chemical reactivity between methacrylic and vinyl monomers [15, 42, 43] and also because of total yield of the polymerizations was not reached. Average molecular weight and M_w/M_n of the copolymers based on HEI were significant lower in comparison to MTOS and MVE, reaching values that are characteristic of the controlled free radical polymerization ($M_w/M_n < 1.5$). This effect is due to the stabilization effect of VI that can react with propagating radicals, leading the formation of stable radicals[44].

Table 1: Feed and copolymer molar fraction, yield of the copolymerization reaction, molecular weight, polydispersity (M_w/M_n) and T_g of poly(VP-*co*-MTOS)(89:11), poly(VP-*co*-MVE)(60:40) and poly(VI-*co*-HEI) copolymers.

Copolymer	**F_{meth}**	**f_{meth}**	**Yield (%)**	**$M_n \cdot 10^{-3}$**	**$M_w \cdot 10^{-3}$**	**M_w/M_n**	**T_{g1} (ºC)**	**T_{g2} (ºC)**

MTOS	0.10	0.11	79	46,8	82,1	1.8	66.0	144.0
MVE	0.15	0.40	59	18,0	29,3	1.9	78.5	143.5
Name	**F_{HEI}**	**f_{HEI}**	**Yield (%)**	**$M_n \cdot 10^{-3}$**	**$M_w \cdot 10^{-3}$**	**M_w/M_n**	**T_g (ºC)**	
HEI-6	0.05	0.06	68	15,9	21,7	1.4	66.6	
HEI-14	0.10	0.14	62	15,6	22,5	1.4	50.5	

NPs characterization

New NPs were synthesized by the combination of MTOS or MVE and HEI-6 or HEI-14 copolymers drugs. **Table 2** includes the most relevant characteristics of these NPs. The characterization of NPs based on HEI6 or HEI14 is included in Figure S2, see *Supporting Information*. D_h varied between 108 and 184 nm with relatively low PDI values, according to the unimodal and narrow size distributions. In particular, these combined NPs presented a lower size in comparison to HEI based NPs, improving their application as drug delivery systems in pro-inflammatory diseases. On the one hand, NPs had a size lower than 200 nm that improves their uptake by cells. On the other hand, NPs presented a D_h higher than 100 nm avoiding their elimination by the RES systems[45].

The size of NPs significantly increased with the HEI content in the copolymer and in the mixture with MTOS and MVE. As an example, the size of MVE-HEI6 based NPs varied from 108 to 161 nm when the feed weight percentage of these different copolymers was increased from 10 to 20 % w/w, respectively (**figure S3A and B,** *see Supporting Information*). At a same feed weight percentage of 90:10, the hydrodynamic diameter also increased as a function of the HEI content in the copolymer, ranging between 108 and 135 nm for HEI6 and HEI14 respectively (**figure S3C and D,** *see Supporting Information*). D_h and PDI were stable as a function of temperature (from 24 to 42ºC (**figure S4,** *see Supporting Information*).

Table 2: Hydrodynamic diameter (D_h), polydispersity index (PDI), zeta potential values (ζ) and Isoelectric point (pI) of the NP based on the combination of poly(VP-*co*-MTOS)(89:11) or poly(VP-*co*-MVE)(60:40) and poly(VI-*co*-HEI)(94:6) or (86:14).

Copol A	**Copol B**	**B (wt-%)**	**D_h (nm)**	**PDI**	**ζ (mV)**	**pI (pH)**
MTOS	HEI6	10	122 ± 8	0.172 ± 0.045	-2.8	5.4

		20	141 ± 3	0.131 ± 0.040	- 3.3	5.8
	HEI14	10	157 ± 10	0.241 ± 0.061	-2.1	4.9
		20	180 ± 17	0.173 ± 0.038	-2.2	5.2
MVE	HEI6	10	108 ± 7	0.090 ± 0.020	-2.1	5.0
		20	161 ± 11	0.093 ± 0.013	-0.5	6.5
	HEI14	10	135 ± 10	0.232 ± 0.062	-3.2	5.9
		20	184 ± 11	0.106 ± 0.074	-2.6	6.5

Although HEI6 and HEI14 based NPs presented positive zeta potentials, the charge of combined NPs were slightly negative. These results indicate the almost neutral charge into the NPs surface. Probably, VI units could be intercalated with a majority number of VP units that are characterized by the absence of charged groups. These results are in the same magnitude order described for other VP nano-assemblies[46, 47].

The pH sensitivity of these combined NPs was proved by the measurement of their pI that was defined as the pH where zeta potential is zero, or the surface charge of the NP is zero. pKa determination by potentiometric titration was not possible due to the low sensitivity of titration curves. **Figure** 1 shows the variation of the zeta potential as a function of pH for NPs based on MTOS or MVE and HEI6 or HEI14, including the effect to vary the weight percentage of these different copolymers (90:10 or 80:20 w:w). It is noteworthy that ζ significantly decreased with the increasing of pH as a result of the conversion of protonated to deprotonated form of VI units that are located into the NP surface. This effect produced a destabilization of self-assembled NPs at basic pH with a strongtendency to their aggregation[48].

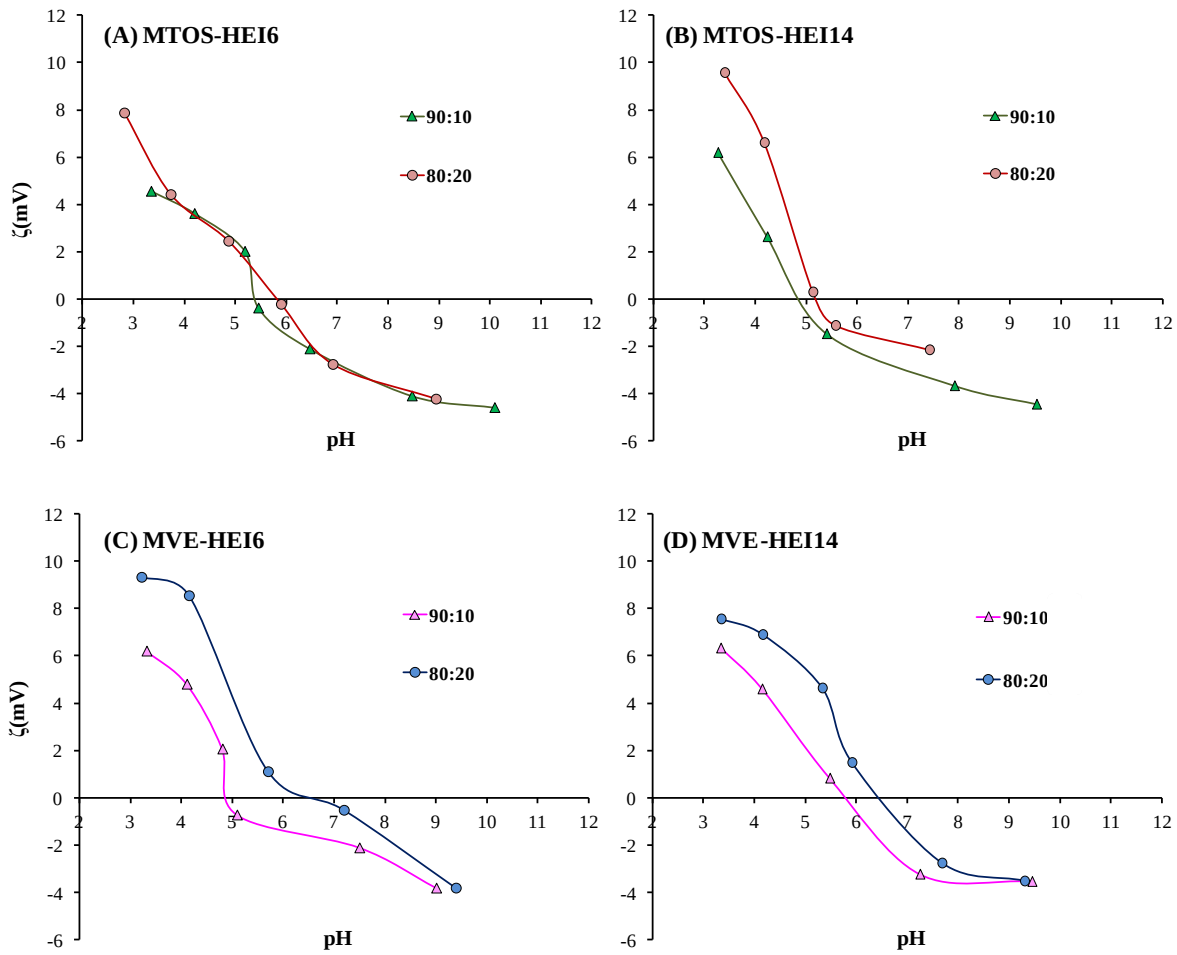

Figure 1: Variation of zeta potential values of NPs based on (A) MTOS-HEI6, (B) MTOS-HEI14, (C) MVE-HEI6 and (D) MVE-HEI14 as a function of pH.

pI of the NPs slightly increased with the content in HEI copolymer, ranging from 5.0 to 6.5. MTOSor MVEwith a 20 wt. % of HEI-based copolymers presented pI values similar to the slightly acid environment. In these conditions, pI of combined NPs were very close to the slightly acid environment of the inner ear exposed to an ototoxic event like CDDP treatment, which enhances the inflammation[49, 50]. For that reason, these NPs were selected to encapsulate Dx and c6 in their inner core. The most characteristic properties of these loaded NPs are summarized in the **table 3**.

Both hydrophobic molecules were successfully entrapped in the nano-assemblies with EE higher than 24% in all copolymeric systems. All size distributions were unimodal with D_h ranging from158to 230 nm and low PDI values. Recently, our group described the encapsulation of MP, Dx or α-TOS in the inner core of MVE or MTOS based NPs. In this case, NPs lower particle size (D_h lower than 160 nm) in comparison to these blend

copolymeric systems. However, the EE in both types of NPs, with or without HEI-based copolymers, was in the same order of magnitude[2, 22] and around two orders of magnitude lower than the conventional intratympanic treatment (Dx, 8 mg, 0.9cc)

All these results confirmed that these copolymeric blend NPs could be excellent candidates for their use as drug delivery systems for the controlled administration of otoprotective drugs or other hydrophobic moleculesthat are quite toxic and also problematic for its effective administration. Nevertheless , the D_h of NPs based on MVE with HEI-based copolymers was near or even higher to the maximum particle size (≥200nm) that is able to cross through RWM[51]. As it will be demostrated in the following sections, this parameter will be crucial to explain the *in vitro* and *in vivo* results of the different nanoformulation tested.

Table 3: Hydrodynamic diameter (D_h), polydispersity index (PDI), zeta potential values (ζ) and Isoelectric point (pI) of the NPs based on the combination of MTOSor MVEand HEI6 or HEI14.

Drug	Copol A	Copol B	Dx (wt-%)	EE (%)	D_h (nm)	ζ (mV)	PDI
Dx	MTOS	HEI-6	10	26	159 ±12	-6.5	0.125 ± 0.016
		HEI-14	10	33	181 ± 11	-5.2	0.138 ± 0.020
		HEI-6	15	24	181 ±18	-3.8	0.114±0.055
		HEI-14	15	25	187.±3	-3.4	0.102±0.028
	MVE	HEI-6	10	59	179 ± 4	-2.6	0.040±0.014
		HEI-14	10	53	211.±36	-0.5	0.108±0.074
		HEI-6	15	36	201±13	-2.5	0.068±0.022
		HEI-14	15	41	230±24	-3.9	0.186±0.068
c6	MTOS	HEI-14	20	----	176 ± 10	- 1.8	0.232 ± 0.046
	MVE	HEI-14	20	----	175 ± 13	- 3.3	0.189 ± 0.028

In vitro release experiments

- *c6 release as a function of pH*

As it was previously demonstrated, the pI of the self-assembled NPs was adjusted to 5.0-6.0 with the aim to promote the VI ionization and therefore the preferential release of the entrapped hydrophobic molecules in the acidic environment promoted by an ototoxic event. c6-loaded NPs were successfully prepared and used as fluorescence probe to check the influence of pH on their fluorescence emission intensity. Results of fluorescence titration of different c6-loaded NPs as a function of pH is shown in the **figure 2**. Additionally, the effect of pH on the particle size of these different formulations is also represented.

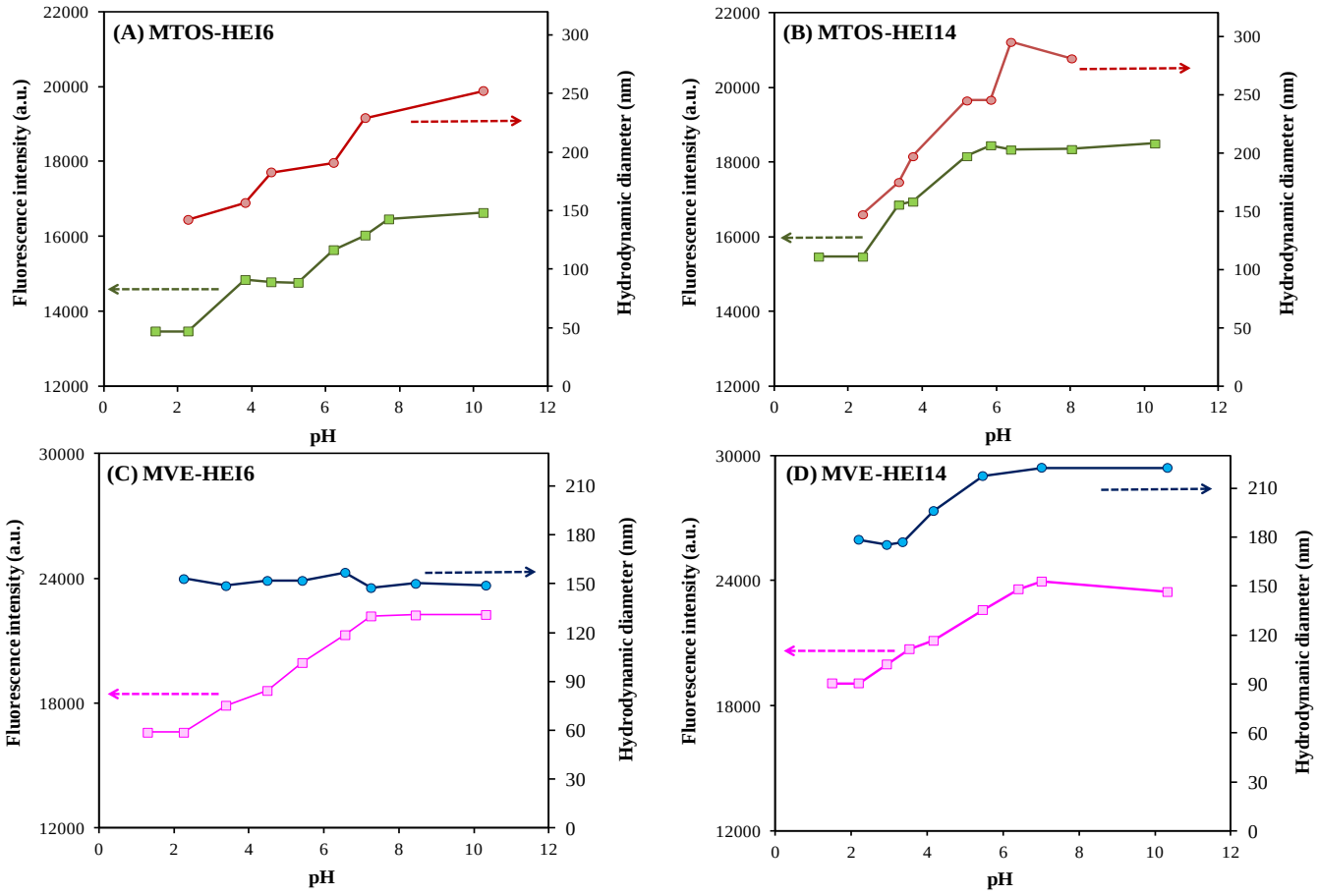

Figure 2. Fluorescence titration and D_h of c6-loaded NPs based on (A) MTOS-HEI6, (B) MTOS-HEI14, (C) MVE-HEI6 and (D) MVE-HEI14 (80:20) copolymeric formulations as a function of pH.

In all cases, the fluorescence emission intensity of coumarin-6 significantly varied as a function as pH due to the protonation of VI units that are located into the NP surface. At very acid pH (lower than pKa of each NPs formulation), protonation of VI units decreased the emission fluorescence intensity. At increasing pH, this emission of coumarin-6 fluorescence significantly increased due to the progressive deprotonation of VI.

In all cases, the transition of emission fluorescence was equivalent to the pI values that were obtained from titration curves. Furthermore, the change of fluorescence was also accompanied by the increasing of hydrodynamic diameter. As it was previously demonstrated, ζ decreased with the increment of pH, producing a destabilization effect that favored the aggregation and therefore the increase of particle size. These results suggest that these pH sensitive NPs significantly enhance the preferential release of hydrophobic molecules in the acidic inflammatory environment in comparison to normal tissues.

- *Esterase mediated Dx release*

In vitro release of Dx was studied by an esterase-mediated dialysis diffusion method. **Figure 3A** shows the *in vitro* Dx release profile of MVE-HEI14-10Dx andMTOS-HEI14-10Dx NPs at 37 °C during 15 days. About 20% of the loaded Dx was released from the MVE-HEI14-10-Dx and more than 45% from MTOS-HEI14-10Dx within fifteen days. Esterase mediated drug release profiles of the systems followed a zero order kinetic during the first 2 weeks, followed by a non-linear period for longer periods of time (**figure 3A**). The biological half-life of Dx in the inner ear is around 8 hours [52]and therefore, Dx sustained release is of great interest to its application as otoprotector of CDDP-induced toxicity[53]. Degradation of the NPs could be seen after 15 days of exposure to esterase, and their size were higher than in the first day (**figure 3B- E**).

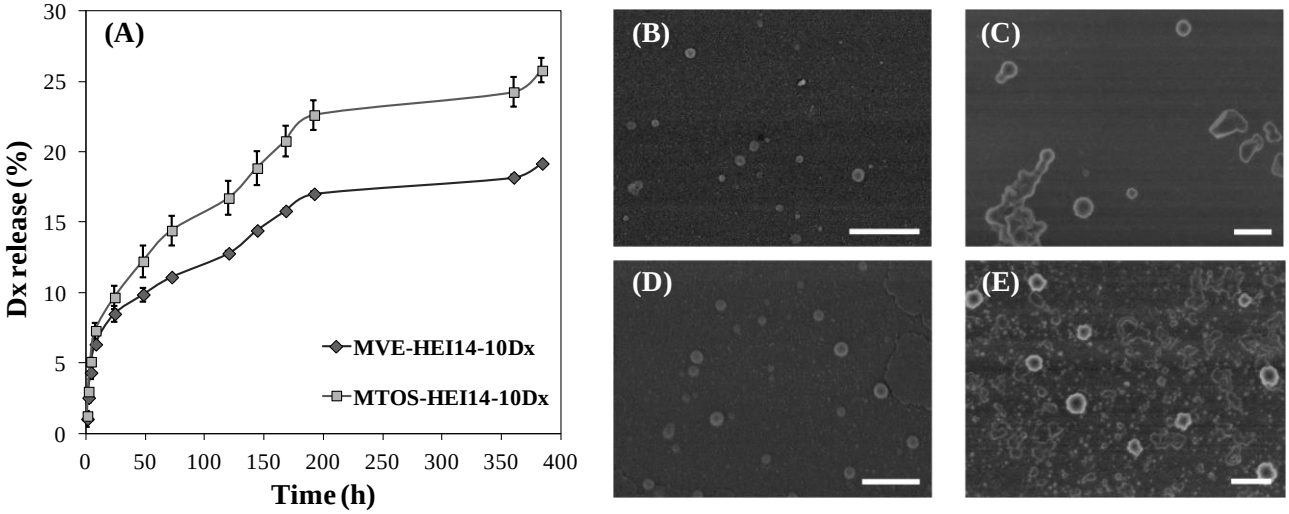

Figure 3: (A) Esterase (15u/ml) mediated *in vitro* release profile of Dx-loaded NPs in PBS at 37 °C. SEM micrographs of MVE-HEI14-10Dx (B) and MTOS-HEI14-10Dx before release (D) and after 15 days of esterase degradation under physiological conditions (C and E respectively).

In vitro biological activity

In vitro biological activity of Dx-loaded NPs based on MTOS or MVE and HEI6 or HEI14 (80:20) was tested using HEI-OC1in order to evaluate their cytoprotection activity against CDDP. The aim of these experiments was to optimize the most appropriate concentration of Dx entrapped NPs that allows combining an optimal anti-apoptotic, antioxidant and anti-inflammatory activity in a same pH-sensitive drug delivery system for otoprotection. As it is shown in **figure 4**, all tested Dx-loaded NPs were non cytotoxicity after 24 hours (viability <70%; ISO 10993−5:2009).

Additionally, after 4h of NPs exposure to HEI-OC1, 30 µM CDDP was added and kept in the cell culture over 24 h. Cell viability decreased between 40 and 50% when 30 µM CDDP was added to the cells (**see figure 5**). Particularly, MTOS-HEI6 NPs reduced CDDP-induced cytotoxicity (almost 10%) but only with a dose of 2.0 mg/ml the difference with CDDP-treated control was statistically significant (**figure 5A**). MVE-HEI6 NPs did not show statistically significant differences with only CDDP treated cells (**figure 5C**). Moreover, MTOS-HEI14 and MVE-HEI14 NPs loaded with 10% w/w of Dx with respect to the polymer were the most effective formulations protecting against CDDP cytotoxicity *in vitro* in a wide range of concentrations (over 20% when treated with MTOS-HEI14 NPs and 15% when treated with MVE-HEI14 at 1 mg/mL and 2

mg/mL, respectively)(**figure 5B and D**). Between 2 and 0.25 mg/ml both formulations significantly reduced CDDP-induced cytotoxicity of 30 µM CDDP.

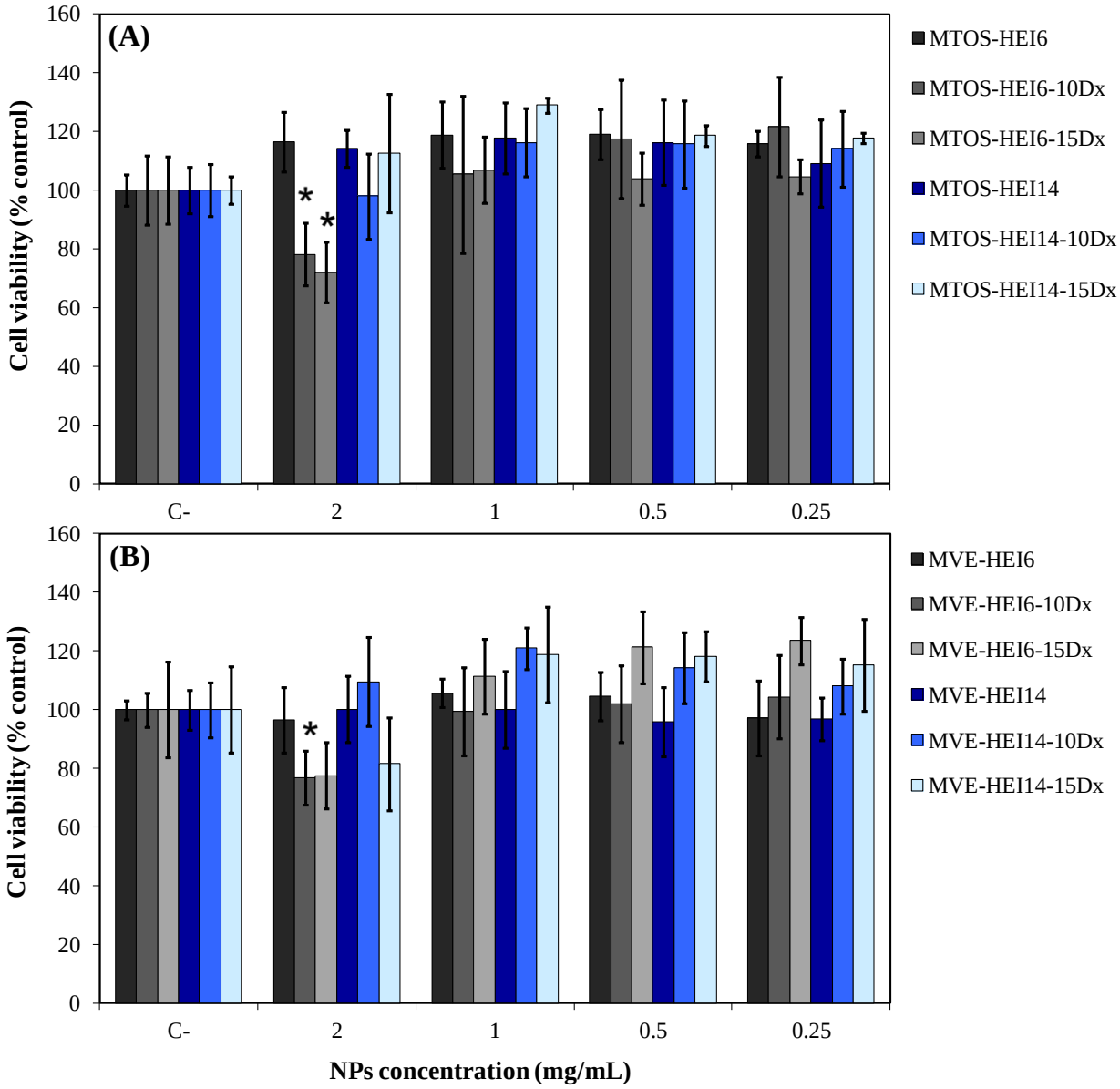

Figure 4: Cell viability of HEI-OC1 treated with different concentrations of Dx-loaded NPs over 24 hours. The diagrams include the mean, the standard deviation (n = 8), and the ANOVA results (*p < 0.05).

Our group previously tested the *in vitro* biological activity of MVE and MTOS-10 Dx NPs. However, these NPs did not show significant differences in comparison to CDDP treated cells[22]. These results confirm that the presence of HEI-based copolymers into the NP systems significantly enhanced their otoprotection activity against CDDP.

The combination of an adequate size and optimal EE could be related with the great results obtained for MTOS-HEI14 systems. However, MVE-HEI14 demonstrated a significant protection against 30μM CDDP dose, even though their sizes were slightly higher than the optimal diameter for this application [51]. D_h higher than 200 nm is not a limiting factor in the internalization or at least the release of the drug to properly reach the cells in the case of MVE-HEI14 NPs. However, this is a key parameter to cross through RWM in the in vivo experiments, as will be explain below[54].

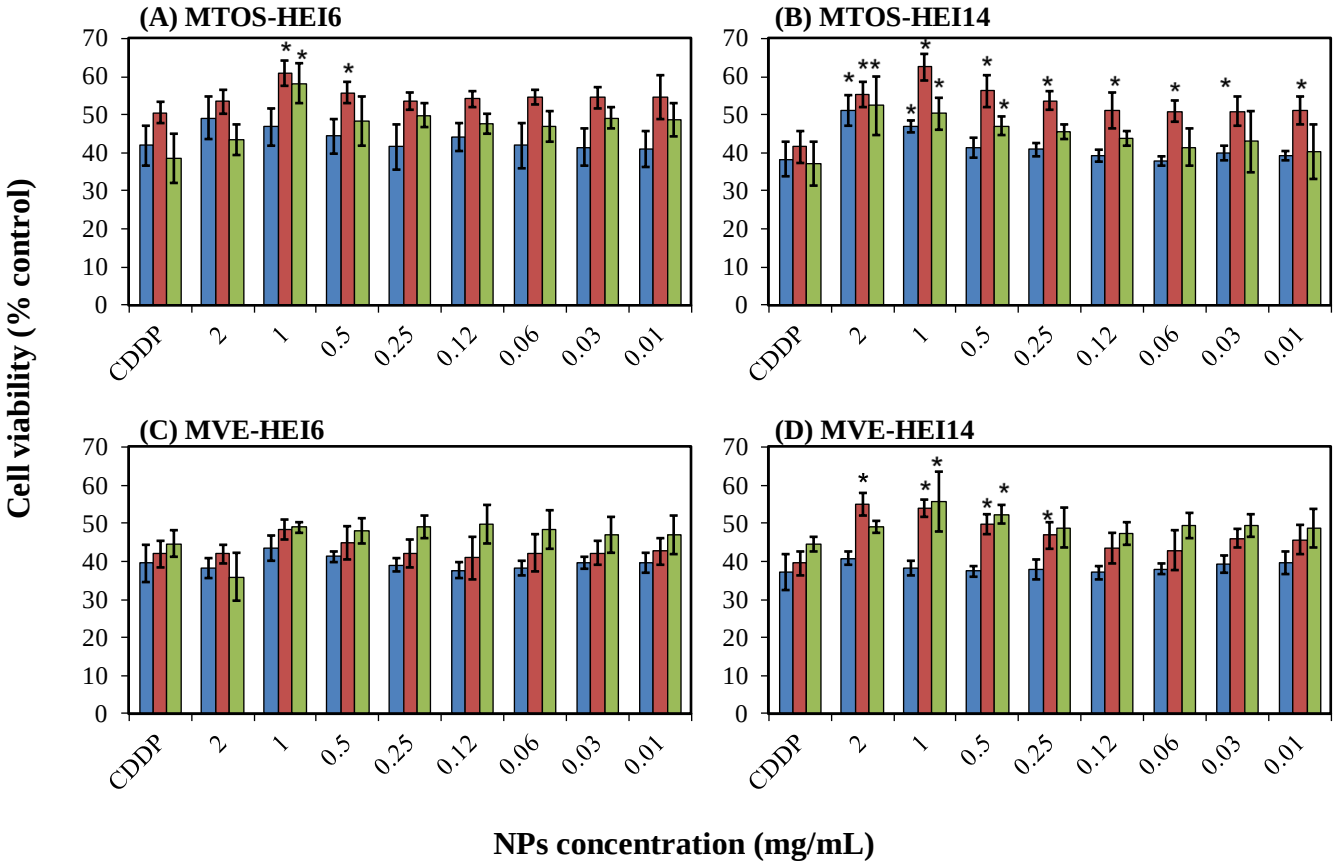

Figure 5: Cell viability of HEI-OC1 treated with different concentrations of MTOS-HEI6 (A) MTOS-HEI14 (B), MVE-HEI6 (C) and MVE-HEI14 (D) NPs, to inhibit the cytotoxic effect of 30 μM CDDP at 24 hours. The diagrams include the mean, the standard deviation (n = 8), and the ANOVA results (*p < 0.05) (legend: unloaded NPs in blue; 10% w/w of Dx in red and 15% w/w of Dx in green).

Biochemical assays

CDDP rapidly causes ototoxicity with a high incidence, resulting in cell death by apoptosis in the inner ear that could be related to the activation of different pathways. One of them involves the activation of caspase-3 which cleaves several substrates resulting in

chromosomal DNA fragmentation and cellular morphologic changes characteristic of apoptosis[55, 56]. In this way, NPs based on MTOS-HEI14-10Dx at 1 mg/ml were able to significantly reduce caspase-3/7 activity in cells treated with CDDP during 16 hours (**figure 6A**). However, MVE-HEI14-10Dx NPs slightly reduced caspase 3/7 activity but not in a statistically significant way, probably due to their higher size and slower Dx release in comparison to NPs based on MTOS-HEI14.

Dx could act as free radical scavenger[57], reducing the IL-1β release and therefore ameliorating ototoxicity in animals receiving CDDP[58]. **Figure 6B** shows theIL-1β release after the treatment with Dx-loaded NPs. In both type of nanoformulations, theIL-1β release was significantly inhibited. In this sense, these polymeric formulations contains a 20% molar of HEI14 copolymer into their composition with demonstrated anti-inflammatory properties [25]. Therefore, the combined action of the entrapped corticoid and the ibuprofen released from the polymer could explain the inhibition of IL-1β release. Downregulation of pro-inflammatory cytokines such as TNF-α, IL-6 and IL-1β, which play a critical role in CDDP ototoxicity, resulted in the attenuation of CDDP-induced cochlear damage [50].

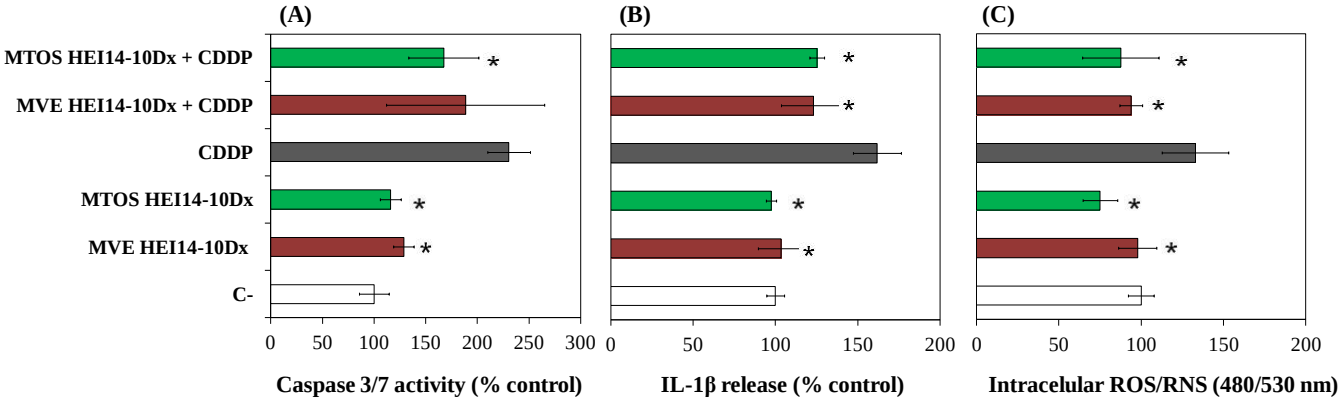

Figure 6: Caspase-3/7 expression when cells were treated with 20 μM CDDP and 0.25 mg/ml NPs suspension at 16 hours (A). IL-1β release after treatment with 20 μM CDDP and 0.25 mg/ml NPs suspension over 24 hours (B). Intracellular ROS measure after treatment with 20 μM CDDP and 0.25 mg/ml NPs suspension over 24 hours (C). The diagrams include the mean, the standard deviation (n = 4), and the ANOVA results (* $p < 0.05$ statistically significant with CDDP).

Finally, it is known that CDDP increased ROS generation in the cochlea in a dose dependent way[9]. CDDP-induced ototoxicity is closely related to the increased production of ROS and that intracellular oxidative stress, could overwhelm the antioxidant defense mechanisms within the cochlea, activating the apoptotic pathway

causing the death of cochlear cells[59]. Both NPs systems efficiently reduced intracellular ROS production respect to CDDP treated cells *in vitro*, even not showing difference with untreated cells (**figure 6C**).

In vivo experiments

In order to maximize NPs delivery to inner ear, the highest dose of NPs (2 mg/ml) was used due to its non toxic effect *in vitro*. NP formulations with best results *in vitro* were selected to *in vivo* assays. Two animals per formulation (MVE-HEI14-10Dx and MTOS-HEI14-10Dx) were inoculated through bullostomy in the right ear. These animals were not treated with CDDP after surgery although they did get the same palliative cares than the animals that received the chemotherapeutic treatment. After 72 hours of both NPs exposure, no significant differences were observed between the auditory thresholds of the right ear and the left ear at all frequencies (**figure 7A-B**).

A potential problem with the administration of antioxidants and corticoids is a reduction in antitumor efficacy of CDDP. That fact was resolved by the bullostomy approach, improving the Dx delivery to the inner ear without systemic interaction in other tissues. Due to CDDP-induced ototoxicity an increase in auditory threshold is shown for frequencies located in the apical turn of the cochlea corresponding to higher frequencies. CDDP entry into cochlear cells results in cell death, which appears to be primarily caspase-dependent[59]. Several mechanism pathways that could trigger to CDDP-induced apoptosis included ROS accumulation which triggers to inflammatory mechanisms that contribute to the cell destruction by up regulation of pro-inflammatory cytokines like TNFα, IL-1β and IL-6[60].

I*n vitro*results suggested the potential of both systems to ameliorate CDDP-induced ototoxicity in a murine model. MTOS-HEI14-10Dx and MVE-HEI14-10Dx were tested *in vivo* and only the first one showed protection against CDDP-induced hearing loss. MTOS-HEI14-10Dx NPs protected in a significant way in most of the measured frequencies (**figure 7C**). NP-MVE-HEI14-10Dx showed no difference between the non-treated left ear and NP treated right ear (**figure 7D**).

EE of Dx in MVE-HEI14-10Dx was substantially higher than in MTOS-HEI14-10Dx. However, MVE-HEI14-10Dx did not protect from CDDP-induced hearing loss *in vivo*. These results could be due to the medium size of this system which is higher than MTOS-

HEI14-10Dx NPs, and was near to the optimal D_h (≥200nm) previously described to cross through RWM[51]. This factor was described as a must to properly deliver of NPs system to cochlear cells from middle ear. Better medium size of MTOS-HEI14-10Dx NPs allowed it to cross RWM and effectively deliver Dx into cochlear cells resulting in the reduction of CDDP-induced hearing loss in all the frequencies measured. This NP system demonstrated statistically significant protection between 16000 and 32000 Hz (**Figure 7C**). In spite of the lower EE showed by MTOS-HEI14-10Dx NP, the physical properties of this system allowed it to an efficient drug delivery to the inner ear.

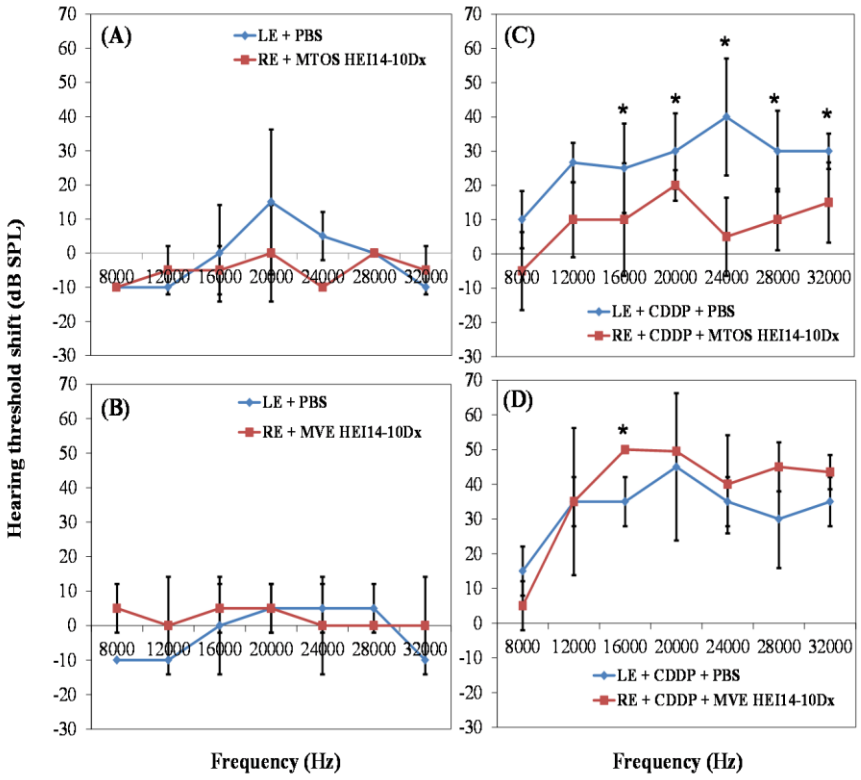

Figure 7: Hearing threshold after local administration by bullostomy in right ear of MTOS-HEI14-10Dx (A) and MVE-HEI14-10Dx (B) NPs (LE: left ear; RE: right ear).Δ of hearing threshold after local administration by bullostomy in right ear of MTOS-HEI14-10Dx (C) and MVEHEI14-10Dx (D) NPs and intraperitoneal 10 mg/kg dose of CDDP (LE: left ear; RE: right ear). The diagrams represents the difference between hearing threshold after CDDP-administration and before treatment with the NP suspension (in the right ear) and CDDP-administration after 72 hours. Diagrams include the mean, the standard deviation (n = 6), and the t-test for pairedsamples were used to compare the variation in ASSR thresholds after treatment, between LE and RE. Values of $p^* < 0.05$ were considered statistically significant.

- *In vivo distribution of c6-loaded NPs*

The green fluorescence of c6 was used to visualize the *in vivo* internalization of MTOS-HEI14 NP into the cochlea, after their administration in the middle ear. As it is shown in

figure 8, MTOS-HEI14-c6 were preferentially accumulated in the basal turn of the cochlea and the intensity of the green fluorescence progressively decreased from the basal to the apical turn.

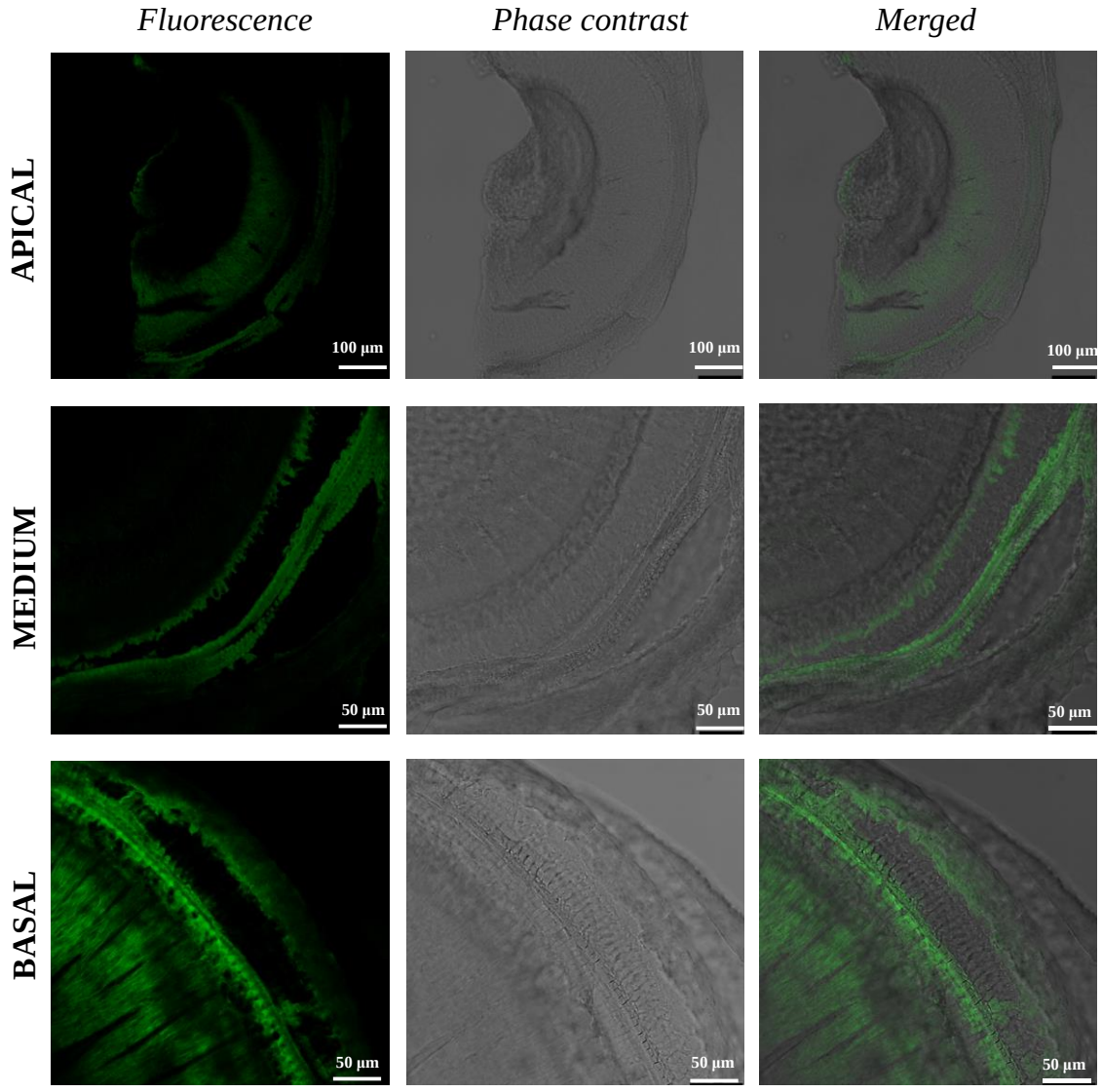

Figure 8: Right ear basal, medium and apical turn of the cochlea an animal treated with c6-loaded MTOS-HEI-14 NPs, including c6 fluorescence, phase contrast and merged images.

Conclusions

The combination of copolymeric drugs obtained by free radical polymerization forming surfactant-free NPs is described for the first time. These nanocarriers were used to efficiently entrapped Dx as anti-inflammatory and anti-apoptotic molecule. The drug was incorporated in the hydrophobic core of NPs and presented good properties *in vitro*. *In*

vitro biological test showed lower CDDP-induced toxicity, down-regulation of caspase 3/7 expression, and lower IL-1β release and intracellular ROS accumulation, while *in vivo* experiments demonstrated a reduced hearing loss when animals received MTOS-HEI14-10Dx NPs. Hydrodynamic diameter of MVE-HEI14-10Dx NPs probably avoid it to cross trough RWM resulting in non protection of the auditory function after CDDP treatment. The local administration of the NPs by bullostomy provided an adequate biological activity locally.

AUTHOR INFORMATION

Corresponding Author

*****Telephone: +34915618806 (ext. 212); Fax: +34915644853; Email: **mraguilar@ictp.csic.es**

Funding Sources

This work was funded by the Spanish Ministry of Economy and Competitiveness (MAT2014-51918-C2-1-R) and CIBER BBN-ECO Foundation project.

Acknowledgments

Authors would like to thank financial support from the Spanish Ministry of Economy and Competitiveness (MAT2014-51918-C2-1-R) and CIBER BBN-ECO Foundation project. Authors also acknowledge, David Gómez, Rosa Ana Ramírez and Mar Fernández for their help in SEM, and cell culture experiments, respectively.

REFERENCES

[1] C.O. Pritz, J. Dudás, H. Rask-Andersen, A. Schrott-Fischer, R. Glueckert, Nanomedicine strategies for drug delivery to the ear, Nanomedicine, 8 (2013) 1155-1172.
[2] S. Martín-Saldaña, R. Palao-Suay, A. Trinidad, M.R. Aguilar, R. Ramírez-Camacho, J. San Román, Otoprotective properties of 6α-methylprednisolone-loaded nanoparticles against cisplatin: In vitro and in vivo correlation, Nanomedicine: Nanotechnology, Biology and Medicine, 12 (2016) 965-976.
[3] J.-Z. Du, X.-J. Du, C.-Q. Mao, J. Wang, Tailor-made dual pH-sensitive polymer–doxorubicin nanoparticles for efficient anticancer drug delivery, Journal of the American Chemical Society, 133 (2011) 17560-17563.
[4] T. Traitel, R. Goldbart, J. Kost, Smart polymers for responsive drug-delivery systems, Journal of Biomaterials Science, Polymer Edition, 19 (2008) 755-767.
[5] M.R. Aguilar, J. Roman, Smart polymers and their applications, Elsevier, 2014.
[6] A. Lardner, The effects of extracellular pH on immune function, Journal of leukocyte biology, 69 (2001) 522-530.
[7] J. Liu, Y. Huang, A. Kumar, A. Tan, S. Jin, A. Mozhi, X.-J. Liang, pH-sensitive nano-systems for drug delivery in cancer therapy, Biotechnology advances, 32 (2014) 693-710.
[8] I. Pyykkö, J. Zou, A. Schrott-Fischer, R. Glueckert, P. Kinnunen, An Overview of Nanoparticle Based Delivery for Treatment of Inner Ear Disorders, Methods in molecular biology (Clifton, NJ), 1427 (2015) 363-415.
[9] R. Marullo, E. Werner, N. Degtyareva, B. Moore, G. Altavilla, S.S. Ramalingam, P.W. Doetsch, Cisplatin induces a mitochondrial-ROS response that contributes to cytotoxicity depending on mitochondrial redox status and bioenergetic functions, PLoS ONE, 8 (2013).
[10] L.P. Rybak, D. Mukherjea, S. Jajoo, V. Ramkumar, Cisplatin ototoxicity and protection: clinical and experimental studies, Tohoku J Exp Med, 219 (2009) 177-186.
[11] D. Fennell, Y. Summers, J. Cadranel, T. Benepal, D. Christoph, R. Lal, M. Das, F. Maxwell, C. Visseren-Grul, D. Ferry, Cisplatin in the modern era: The backbone of first-line chemotherapy for non-small cell lung cancer, Cancer treatment reviews, 44 (2016) 42-50.
[12] L.H. Einhorn, Curing metastatic testicular cancer, Proceedings of the National Academy of Sciences, 99 (2002) 4592-4595.
[13] T. Karasawa, P.S. Steyger, An integrated view of cisplatin-induced nephrotoxicity and ototoxicity, Toxicology letters, 237 (2015) 219-227.
[14] D. Mukherjea, S. Jajoo, K. Sheehan, T. Kaur, S. Sheth, J. Bunch, C. Perro, L.P. Rybak, V. Ramkumar, NOX3 NADPH oxidase couples transient receptor potential vanilloid 1 to signal transducer and activator of transcription 1-mediated inflammation and hearing loss, Antioxidants & redox signaling, 14 (2011) 999-1010.
[15] M.L. Donaire, J. Parra-Cáceres, B. Vázquez-Lasa, I. García-Álvarez, A. Fernández-Mayoralas, A. López-Bravo, J. San Román, Polymeric drugs based on bioactive glycosides for the treatment of brain tumours, Biomaterials, 30 (2009) 1613-1626.
[16] L. García-Fernández, S. Halstenberg, R.E. Unger, M.R. Aguilar, C.J. Kirkpatrick, J. San Román, Anti-angiogenic activity of heparin-like polysulfonated polymeric drugs in 3D human cell culture, Biomaterials, 31 (2010) 7863-7872.
[17] F. Reyes-Ortega, G. Rodríguez, M.R. Aguilar, M. Lord, J. Whitelock, M.H. Stenzel, J. San Román, Encapsulation of low molecular weight heparin (bemiparin) into

polymeric nanoparticles obtained from cationic block copolymers: properties and cell activity, Journal of Materials Chemistry B, 1 (2013) 850-860.
[18] J. Neuzil, T. Weber, N. Gellert, C. Weber, Selective cancer cell killing by α-tocopheryl succinate, British journal of cancer, 84 (2001) 87.
[19] N. Duhem, F. Danhier, V. Préat, Vitamin E-based nanomedicines for anti-cancer drug delivery, Journal of Controlled Release, 182 (2014) 33-44.
[20] L.-F. Dong, P. Low, J.C. Dyason, X.-F. Wang, L. Prochazka, P.K. Witting, R. Freeman, E. Swettenham, K. Valis, J. Liu, α-Tocopheryl succinate induces apoptosis by targeting ubiquinone-binding sites in mitochondrial respiratory complex II, Oncogene, 27 (2008) 4324-4335.
[21] R. Palao-Suay, M.R. Aguilar, F.J. Parra-Ruiz, M. Fernández-Gutiérrez, J. Parra, C. Sánchez-Rodríguez, R. Sanz-Fernández, L. Rodrigáñez, J.S. Román, Anticancer and Antiangiogenic Activity of Surfactant-Free Nanoparticles Based on Self-Assembled Polymeric Derivatives of Vitamin E: Structure–Activity Relationship, Biomacromolecules, 16 (2015) 1566-1581.
[22] S. Martín-Saldaña, R. Palao-Suay, M.R. Aguilar, R. Ramírez-Camacho, J. San Román, Polymeric nanoparticles loaded with dexamethasone or α-tocopheryl succinate to prevent cisplatin-induced ototoxicity, Acta Biomaterialia, 53 (2017) 199-210.
[23] S.K. Kim, G.J. Im, Y.S. An, S.H. Lee, H.H. Jung, S.Y. Park, The effects of the antioxidant α-tocopherol succinate on cisplatin-induced ototoxicity in HEI-OC1 auditory cells, International journal of pediatric otorhinolaryngology, 86 (2016) 9-14.
[24] B. Li, K. Su, G. Yang, Y. Feng, L. Xia, S. Yin, Assessment of the Potential Ototoxicity of High-Dose Celecoxib, a Selective Cyclooxygenase-2 Inhibitor, in Rats, Otolaryngology--Head and Neck Surgery, 152 (2015) 1108-1112.
[25] P. Suárez, L. Rojo, Á. González-Gómez, J.S. Román, Self-Assembling Gradient Copolymers of Vinylimidazol and (Acrylic) ibuprofen With Anti-Inflammatory and Zinc Chelating Properties, Macromolecular bioscience, 13 (2013) 1174-1184.
[26] D. Velasco, G. Réthoré, B. Newland, J. Parra, C. Elvira, A. Pandit, L. Rojo, J. San Román, Low polydispersity (N-ethyl pyrrolidine methacrylamide-co-1-vinylimidazole) linear oligomers for gene therapy applications, European Journal of Pharmaceutics and Biopharmaceutics, 82 (2012) 465-474.
[27] A.B.E. Attia, Z.Y. Ong, J.L. Hedrick, P.P. Lee, P.L.R. Ee, P.T. Hammond, Y.-Y. Yang, Mixed micelles self-assembled from block copolymers for drug delivery, Current opinion in colloid & interface science, 16 (2011) 182-194.
[28] D.A. Chiappetta, A. Sosnik, Poly (ethylene oxide)–poly (propylene oxide) block copolymer micelles as drug delivery agents: improved hydrosolubility, stability and bioavailability of drugs, European Journal of Pharmaceutics and Biopharmaceutics, 66 (2007) 303-317.
[29] C.-F. Mu, P. Balakrishnan, F.-D. Cui, Y.-M. Yin, Y.-B. Lee, H.-G. Choi, C.S. Yong, S.-J. Chung, C.-K. Shim, D.-D. Kim, The effects of mixed MPEG–PLA/Pluronic® copolymer micelles on the bioavailability and multidrug resistance of docetaxel, Biomaterials, 31 (2010) 2371-2379.
[30] C. Wu, R. Ma, H. He, L. Zhao, H. Gao, Y. An, L. Shi, Fabrication of complex micelles with tunable shell for application in controlled drug release, Macromolecular bioscience, 9 (2009) 1185-1193.
[31] M. Liu, J. Fu, J. Li, L. Wang, Q. Tan, X. Ren, Z. Peng, H. Zeng, Preparation of tri-block copolymer micelles loading novel organoselenium anticancer drug BBSKE and study of tissue distribution of copolymer micelles by imaging in vivo method, International journal of pharmaceutics, 391 (2010) 292-304.

[32] J. Lin, J. Zhu, T. Chen, S. Lin, C. Cai, L. Zhang, Y. Zhuang, X.-S. Wang, Drug releasing behavior of hybrid micelles containing polypeptide triblock copolymer, Biomaterials, 30 (2009) 108-117.
[33] D. Kim, Z.G. Gao, E.S. Lee, Y.H. Bae, In vivo evaluation of doxorubicin-loaded polymeric micelles targeting folate receptors and early endosomal pH in drug-resistant ovarian cancer, Molecular pharmaceutics, 6 (2009) 1353-1362.
[34] R.R. Sawant, R.M. Sawant, V.P. Torchilin, Mixed PEG–PE/vitamin E tumor-targeted immunomicelles as carriers for poorly soluble anti-cancer drugs: improved drug solubilization and enhanced in vitro cytotoxicity, European Journal of Pharmaceutics and Biopharmaceutics, 70 (2008) 51-57.
[35] Z. Zhang, S. Tan, S.-S. Feng, Vitamin E TPGS as a molecular biomaterial for drug delivery, Biomaterials, 33 (2012) 4889-4906.
[36] R. Vakil, G.S. Kwon, Poly (ethylene glycol)-b-poly (ε-caprolactone) and PEG-phospholipid form stable mixed micelles in aqueous media, Langmuir, 22 (2006) 9723-9729.
[37] C.-M.J. Hu, L. Zhang, Nanoparticle-based combination therapy toward overcoming drug resistance in cancer, Biochemical pharmacology, 83 (2012) 1104-1111.
[38] S. Bin, N. Zhou, J. Pan, F. Pan, X.-F. Wu, Z.-H. Zhou, Nano-carrier mediated co-delivery of methyl prednisolone and minocycline for improved post-traumatic spinal cord injury conditions in rats, Drug Development and Industrial Pharmacy, 43 (2017) 1033-1041.
[39] H.-Z. Li, S.-H. Ma, H.-M. Zhang, J.-M. Liu, Y.-X. Wu, P.-Q. Cao, X. Gao, Nano carrier mediated co-delivery of dapsone and clofazimine for improved therapeutic efficacy against tuberculosis in rats, Biomedical Research, 28 (2017).
[40] X. Duan, J. Xiao, Q. Yin, Z. Zhang, H. Yu, S. Mao, Y. Li, Smart pH-sensitive and temporal-controlled polymeric micelles for effective combination therapy of doxorubicin and disulfiram, ACS nano, 7 (2013) 5858-5869.
[41] H. Fessi, F. Puisieux, J.P. Devissaguet, N. Ammoury, S. Benita, Nanocapsule formation by interfacial polymer deposition following solvent displacement, International journal of pharmaceutics, 55 (1989) R1-R4.
[42] M. Sánchez-Chaves, G. Martínez, E. López Madruga, C. Fernández-Monreal, Synthesis of statistical glycidyl methacrylate-n-vinyl pyrrolidone copolymers and their reaction with naproxen, Journal of Polymer Science Part A: Polymer Chemistry, 40 (2002) 1192-1199.
[43] M. Hurtgen, A. Debuigne, C.-A. Fustin, C. Jérôme, C. Detrembleur, Organometallic-mediated radical polymerization: unusual route toward (quasi-) diblock graft copolymers starting from a mixture of monomers of opposed reactivity, Macromolecules, 44 (2011) 4623-4631.
[44] C. Bamford, E. Schofield, Non-classical free-radical polymerization: Degradative addition to monomer in the polymerization of 1-vinylimidazole, Polymer, 22 (1981) 1227-1235.
[45] F. Danhier, O. Feron, V. Préat, To exploit the tumor microenvironment: Passive and active tumor targeting of nanocarriers for anti-cancer drug delivery, Journal of Controlled Release, 148 (2010) 135-146.
[46] Z. Zhu, Y. Li, X. Li, R. Li, Z. Jia, B. Liu, W. Guo, W. Wu, X. Jiang, Paclitaxel-loaded poly (N-vinylpyrrolidone)-b-poly (ε-caprolactone) nanoparticles: preparation and antitumor activity in vivo, Journal of Controlled Release, 142 (2010) 438-446.
[47] R. Palao-Suay, L. Rodrigáñez, M.R. Aguilar, C. Sánchez-Rodríguez, F. Parra, M. Fernández, J. Parra, J. Riestra-Ayora, R. Sanz-Fernández, J.S. Román, Mitochondrially

Targeted Nanoparticles Based on α-TOS for the Selective Cancer Treatment, Macromolecular bioscience, (2015).
[48] E.S. Lee, K. Na, Y.H. Bae, Super pH-sensitive multifunctional polymeric micelle, Nano Letters, 5 (2005) 325-329.
[49] K. Watanabe, S. Inai, K. Jinnouchi, S. Bada, A. Hess, O. Michel, T. Yagi, Nuclear-factor kappa B (NF-kappa B)-inducible nitric oxide synthase (iNOS/NOS II) pathway damages the stria vascularis in cisplatin-treated mice, Anticancer research, 22 (2001) 4081-4085.
[50] H. So, H. Kim, Y. Kim, E. Kim, H.-O. Pae, H.-T. Chung, H.-J. Kim, K.-B. Kwon, K.-M. Lee, H.-Y. Lee, Evidence that cisplatin-induced auditory damage is attenuated by downregulation of pro-inflammatory cytokines via Nrf2/HO-1, Journal of the Association for Research in Otolaryngology, 9 (2008) 290-306.
[51] G.L. Hornyak, Nanotechnology in otolaryngology, Otolaryngologic Clinics of North America, 38 (2005) 273-293.
[52] L.S. Parnes, A.H. Sun, D.J. Freeman, Corticosteroid pharmacokinetics in the inner ear fluids: an animal study followed by clinical application, The Laryngoscope, 109 (1999) 1-17.
[53] X.W. Teng, N.M. Davies, C. Fukuda, R.L. Good, M.W. Fariss, Pharmacokinetics and tissue distribution of d-alpha-tocopheryl succinate formulations following intravenous administration in the rat, Biopharmaceutics & drug disposition, 26 (2005) 195-203.
[54] A. Punnia-Moorthy, Evaluation of pH changes in inflammation of the subcutaneous air pouch lining in the rat, induced by carrageenan, dextran and Staphylococcus aureus, Journal of Oral Pathology & Medicine, 16 (1987) 36-44.
[55] R. N Abi-Hachem, A. Zine, T. R Van De Water, The injured cochlea as a target for inflammatory processes, initiation of cell death pathways and application of related otoprotective strategies, Recent patents on CNS drug discovery, 5 (2010) 147-163.
[56] L.P. Rybak, C.A. Whitworth, D. Mukherjea, V. Ramkumar, Mechanisms of cisplatin-induced ototoxicity and prevention, Hearing research, 226 (2007) 157-167.
[57] E. Niki, Role of vitamin E as a lipid-soluble peroxyl radical scavenger: in vitro and in vivo evidence, Free Radical Biology and Medicine, 66 (2014) 3-12.
[58] M. Paksoy, E. Ayduran, A. Şanlı, M. Eken, S. Aydın, Z.A. Oktay, The protective effects of intratympanic dexamethasone and vitamin E on cisplatin-induced ototoxicity are demonstrated in rats, Medical Oncology, 28 (2011) 615-621.
[59] L.P. Rybak, V. Ramkumar, Ototoxicity, Kidney Int, 72 (2007) 931-935.
[60] C. Casares, R. Ramirez-Camacho, A. Trinidad, A. Roldan, E. Jorge, J.R. Garcia-Berrocal, Reactive oxygen species in apoptosis induced by cisplatin: review of physiopathological mechanisms in animal models, Eur Arch Otorhinolaryngol, 269 (2012) 2455-2459.